

# 1           **Novel method for quantifying AhR-ligand binding affinities using**

## 2                                       **Microscale Thermophoresis**

3   Anne Stinn<sup>1,2</sup>, Jens Furkert<sup>3</sup>, Stefan H.E. Kaufmann<sup>1,4,5</sup>, Pedro Moura-Alves<sup>1,6\*</sup>, Michael  
4   Kolbe<sup>2,7\*</sup>.

### 6   **Affiliations:**

7   <sup>1</sup>Department of Immunology, Max Planck Institute for Infection Biology, Charitéplatz 1, 10117  
8   Berlin, Germany.

9   <sup>2</sup>Department of Structural Infection Biology, Center for Structural Systems Biology (CSSB),  
10   Helmholtz-Center for Infection Research (HZI), Notkestrasse 85, 22607 Hamburg, Germany.

11   <sup>3</sup>Leibniz-Institut für Molekulare Pharmakologie (FMP), Robert-Rössle-Strasse 10, 13125  
12   Berlin, Germany.

13   <sup>4</sup>Hagler Institute for Advanced Study at Texas A&M University, College Station, TX 7843

14   <sup>5</sup>Max Planck Institute for Biophysical Chemistry, Am Faßberg 11, 37077 Göttingen, Germany.

15   <sup>6</sup>Ludwig Institute for Cancer Research, Nuffield Department of Clinical Medicine, University  
16   of Oxford, OX3 7DQ Oxford, UK.

17   <sup>7</sup>Faculty of Mathematics, Informatics and Natural Sciences, University of Hamburg,  
18   Rothenbaumchaussee 19, 20148 Hamburg, Germany.

19  
20   \*Corresponding author: [pedro.mouraalves@ludwig.ox.ac.uk](mailto:pedro.mouraalves@ludwig.ox.ac.uk), [21   \[hamburg.de\]\(http://hamburg.de\)](mailto:michael.kolbe@cssb-</a></p></div><div data-bbox=)

22

## 23 **Abstract**

24           The aryl hydrocarbon receptor (AhR) is a highly conserved cellular sensor of a variety  
25 of environmental pollutants and dietary-, cell- and microbiota-derived metabolites with  
26 important roles in fundamental biological processes. Deregulation of the AhR pathway is  
27 implicated in several diseases, including autoimmune diseases and cancer, rendering AhR a  
28 promising target for drug development and host-directed therapy. The pharmacological  
29 intervention of AhR processes requires detailed information about the ligand binding properties  
30 to allow specific targeting of a particular signalling process without affecting the remaining.  
31 Here, we present a novel microscale thermophoresis-based approach to monitoring the binding  
32 of purified recombinant human AhR to its natural ligands in a cell-free system. This approach  
33 facilitates a precise identification and characterization of unknown AhR ligands and represents  
34 a screening strategy for the discovery of potential selective AhR modulators.

35

## 36 **Keywords**

37           AhR/recombinant expression/ligand binding/MST/high-throughput screening.

38

## 39 **Introduction**

40           Biomolecular interactions like protein-protein or protein-ligand interactions play an  
41 important role in almost all physiological processes. Remarkably, receptor agonist or  
42 antagonist interactions are of highest interest for the pharmaceutical drug development, where  
43 a detailed investigation of such processes is essential not only for understanding the underlying  
44 molecular mechanisms, but also the mode of action of a drug<sup>1</sup>. Quantitative binding studies can  
45 be performed by a number of biophysical approaches, such as surface plasmon resonance  
46 (SPR) or isothermal titration calorimetry (ITC)<sup>2,3</sup>. However, these techniques are often limited  
47 either due to the immobilization of one of the interaction partners that may interfere with

48 binding (SPR) or due to high sample consumptions (ITC), respectively. Microscale  
49 thermophoresis (MST) is a relatively new method that allows for a fast and robust evaluation  
50 of biomolecular interactions in any desired buffer, including cell lysates or blood serum,  
51 without the need of surface immobilization or the use of excessive protein concentrations<sup>4,5</sup>.

52 The evolutionary highly conserved aryl hydrocarbon receptor (AhR) is a ligand-  
53 dependent transcription factor that mediates responses to environmental pollutants as well as  
54 dietary-, cell- and microbiota-derived metabolites<sup>6</sup>. Although originally identified as dioxin  
55 receptor, extensive research in the last years has demonstrated that the receptor is a key  
56 regulator of a broad spectrum of physiologically relevant functions, spanning from xenobiotic  
57 metabolism, developmental biology, as well as immunity<sup>7-10</sup>. Notably, its high relevance in the  
58 immune response of vertebrates, as well as the involvement in the onset of pathological  
59 conditions, e.g. cancer and autoimmune diseases, makes the AhR a promising target for drug  
60 development and host-directed therapy (HDT)<sup>7,9,11</sup>. As a member of the basic helix-loop-helix  
61 PER-ARNT-SIM (bHLH-PAS) protein family of transcriptional regulators, the AhR is  
62 characterized by a modular organization of regulatory domains, comprising an amino-terminal  
63 bHLH DNA binding domain that is contiguous to a tandem PAS A and PAS B domain<sup>6,7</sup> (Fig  
64 1a). The PAS B domain encompasses the receptors ligand-binding capability<sup>6</sup>. While the AhR  
65 domain architecture and the multifarious interactions with various proteins that enable the  
66 activation of different signalling pathways are well described<sup>6,7</sup>, little is known about the  
67 molecular processes of AhR ligand recognition. This is mainly because the crystal structure of  
68 the PAS B ligand-binding domain still remains to be solved. Moreover, although numerous  
69 AhR ligand binding analyses have been reported in the literature, in their majority radioligand  
70 competition assays and others are focusing on murine and rat AhR or species other than  
71 human<sup>13,14,15</sup>. Up to date, the lack of a robust recombinant expression system that allows for  
72 high-level production of functional human AhR has limited the development of a reliable and

73 sensitive ligand binding assay that enables quantitative measurements of ligand binding  
74 affinities. Currently used methods (e.g. virtual ligand screening combined with AhR reporter  
75 cell studies or enzymatic activities) often result in divergent values, are time-consuming and  
76 do not allow for determination of direct binding, which is a critical aspect in drug discovery<sup>16,17</sup>.  
77 Therefore, we aimed to establish a robust protocol that allows for testing binding affinities of  
78 a purified recombinant human AhR to small molecules by using MST.

79

## 80 **Results and discussion**

### 81 **Recombinant AhR-ARNT is functionally active**

82 In the past, numerous attempts to produce soluble AhR protein comprising the PAS B  
83 ligand-binding domain in sufficient amounts to support structural and functional studies  
84 failed<sup>18,19</sup>. Similarly, we observed that the expression of human AhR (hAhR) in *E. coli* and  
85 mammalian cells resulted exclusively in aggregated and/or insoluble protein material. This was  
86 irrespective of the expression construct and the AhR amino acid boundaries tested (data not  
87 shown). In contrast, several protocols describe the successful expression and purification of the  
88 aryl hydrocarbon nuclear translocator (ARNT)<sup>20,21</sup>. ARNT, also belonging to the bHLH-PAS  
89 protein family, sharing its typical domain architecture, is the interacting partner of AhR that  
90 was shown to dimerize and stabilize the AhR conformation upon ligand binding and receptor  
91 activation<sup>6,21</sup>. We, therefore, decided to make use of this properties and co-expressed the human  
92 AhR (hAhR<sub>23-475</sub>) comprising the ligand-binding domain in complex with murine ARNT  
93 (mARNT<sub>85-465</sub>) in *E. coli* BL21(DE3) (for details see Methods, Fig. 1b and Supplementary Fig.  
94 1). Both proteins were expressed as C-terminal truncations as the C-terminal transactivation  
95 domain is not required for ligand binding and is known to have a tendency to aggregate<sup>6</sup>. To  
96 enhance AhR solubility upon bacterial expression, the protein was fused to an N-terminal FleB  
97 expression tag derived from the *Yersinia enterocolitica* flagellin FliC/FljB, which was shown

98 to be monomeric and expressed at high levels in *E. coli*<sup>22</sup>. Noteworthy, fusion to the N-terminal  
99 solubility tag together with expression in presence of mARNT not only enhanced the  
100 expression levels of hAhR but also resulted in a significantly increased solubility of the  
101 receptor protein (Fig. 1b). This ultimately allowed us to purify sufficient amounts of  
102 recombinant hAhR in complex with mARNT to be further subjected to functional analyses  
103 (Fig. 1b, Supplementary Fig. 1). We initially validated the functionality of the purified protein  
104 complex employing the conventional cell-based radioligand binding assay<sup>18</sup> (Fig. 1c). In this,  
105 an equilibrium dissociation constant ( $K_d$ ) of 2.7-4.2 nM was ascertained for the bona fide ligand  
106 2,3,7,8-tetrachlorodibenzodioxin (TCDD) to the endogenous hAhR in hepatocyte cell lysates<sup>13</sup>.  
107 We assessed the specific binding of radioactively labelled [<sup>3</sup>H]TCDD tracer to the recombinant  
108 AhR-ARNT receptor in the presence of liver lysates derived from AhR deficient mice.  
109 Saturation binding experiments verified the direct binding of the prototypical ligand TCDD to  
110 the purified AhR-ARNT complex with a calculated  $K_d$  of  $39 \pm 20$  nM, and a maximal binding  
111 capacity ( $B_{max}$ ) of  $60.3 \pm 17.3$  pmoles/mg protein (Fig. 1d). The observed binding was specific  
112 to hAhR, as we did not detect any interaction between the individually purified mARNT protein  
113 and [<sup>3</sup>H]TCDD (Supplementary Fig. 2)<sup>20</sup>.

114 Next, we performed competition radioligand binding experiments to evaluate the binding  
115 ability of the recombinant AhR-ARNT to diverse AhR ligands belonging to different structural  
116 classes (Fig. 1e). The bacterial pigment 1-hydroxyphenazine (1-HP) from *Pseudomonas*  
117 *aeruginosa*, previously identified by our group as a potent AhR activator<sup>8</sup>, was chosen as a  
118 representative of microbe-derived AhR ligands. CH-223191, a commercially available AhR-  
119 inhibitor<sup>23</sup>, was chosen as AhR antagonist. We observed a concentration-dependent  
120 displacement of the tracer for both 1-HP and CH-223191, with specific  $K_i$ 's of 9.2  $\mu$ M (95%  
121 confidence limit: 7.4-11.1  $\mu$ M) and 12.2  $\mu$ M (95% confidence limit: 1.8-76.1  $\mu$ M),  
122 respectively, validating the functional activity of the recombinant AhR-ARNT complex in

123 terms of its capability to bind small molecules. Further, we tested the binding affinity of the  
124 endogenous AhR agonist 6-formylindolo-[3,2-b]-carbazole (FICZ)<sup>6,7,24</sup> and the prototypical  
125 exogenous ligand TCDD to AhR in competition binding assays (Fig. 1e). Though reported to  
126 have an affinity in the pM-nM range, we failed to see competition when incubating the purified  
127 AhR-ARNT with increasing concentrations of unlabeled FICZ, which was likely attributed to  
128 the high instability of its tryptophan group in aqueous solution<sup>25</sup>. However, in agreement with  
129 the data obtained from our radioligand saturation experiments, we observed only an initial  
130 competition of unlabeled TCDD for binding to hAhR at the highest concentration. Full  
131 displacement of the radioligand would require the use of even higher concentrations of  
132 unlabeled TCDD, which due to its insolubility in water<sup>26</sup> is not feasible in this experimental  
133 set-up.

134

### 135 **MST is a sensitive method to determine AhR-ligand binding affinities**

136 The radioligand binding assay, although commonly used, is known to be extremely  
137 sensitive to minor changes in the protocol that likely lead to marked differences in the measured  
138 affinities<sup>13,18,26</sup>. Here, total cytosolic extracts of hepatocytes are being used; therefore, the  
139 observed ligand binding may not be specific to AhR, but potentially also arise from unspecific  
140 interactions of the ligand with other constituents of the cytosol. Additionally, due to high  
141 background noise in this assay, only subtle differences in radioactivity can be measured<sup>8,18</sup>.  
142 Thus, the limit and detection range for analyzing specific binding is quite small, which urges  
143 the development of an improved AhR ligand binding assay that can replace the classical  
144 radioligand method.

145 We implemented an MST based assay, which in addition to the low protein amount  
146 required and short assay times, is also characterized by its buffer independency, enabling the  
147 analysis of the receptor under close-to-native conditions. Exploiting the intrinsic fluorescence

148 of proteins, it allows the analysis of biomolecular interactions without the need for sample  
149 modifications due to labelling (Fig. 2a)<sup>5,27</sup>. To evaluate the feasibility of the label-free MST  
150 approach for analyzing small molecule binding to AhR, we first tested the binding of TCDD  
151 to purified AhR-ARNT complexes (Fig. 2b). We titrated the non-fluorescent ligand to a given  
152 concentration of AhR-ARNT complex (250 nM final). Concentration-dependent ligand-  
153 induced differences were readily recorded in the MST traces using AhR-ARNT, but not when  
154 mARNT was used alone, validating the specific binding of TCDD to hAhR (Supplementary  
155 Fig. 3). AhR binding affinity to TCDD was calculated ( $K_d$  of  $139 \pm 99$  nM) (Fig. 2b). Next, we  
156 elucidated the compatibility of MST for analyzing binding of the recombinant AhR-ARNT to  
157 small molecules of various classes (Fig. 2c-e). In contrast to the radioligand binding assay, we  
158 were able to measure specific saturable binding of hAhR to the labile high-affinity agonist  
159 FICZ with a computed binding affinity of  $79 \pm 36$  nM. Employing the same setup, we further  
160 confirmed binding of 1-HP and CH-223191 with binding affinities in the higher nM range with  
161  $K_d$ 's of  $943 \pm 176$  nM and  $496 \pm 82$  nM, respectively. Together, this validated the suitability  
162 of the devised approach for measuring binding of recombinant AhR-ARNT complexes not only  
163 to AhR activators such as 1-HP (Fig. 2c,d) but also to specific inhibitors such as the CH-223191  
164 (Fig. 2e).

165

## 166 **Conclusion**

167 Traditionally, AhR binding assays have been done using radiolabeled ligands as the method  
168 of choice<sup>13,14,18</sup>. However, not only because of the undesirable usage of radioactive and toxic  
169 tracer material, the use of animals for organ extraction and the increased costs involved but  
170 also due to diverse technical reasons, there is a necessity for the development of an improved  
171 ligand binding assay. Besides the apparent sensitivity towards amendments in the protocol,  
172 some studies stress the fact that the radioligand binding assay largely suffers from the

173 insolubility of TCDD and other AhR ligands in water<sup>25,26</sup>. Due to their lipophilic nature, these  
174 compounds are usually dissolved in DMSO. At high concentrations, dilution with the assay  
175 buffer results in precipitation and unspecific interactions of the small molecule candidates with  
176 hydrophobic surfaces, thereby affecting the final results. Yet, the development of a precise and  
177 sensitive AhR ligand binding assay was limited due to the lack of an expression system yielding  
178 high amounts of functional AhR protein. This study demonstrates that the recombinant  
179 expression of hAhR fused to an N-terminal FleB-tag and in complex with its interacting partner  
180 ARNT ultimately allows the purification of significant amounts of functionally active human  
181 receptor protein with yields of 1 mg protein per litre expression culture. Further, the purified  
182 protein is suitable for analyzing receptor-ligand interactions using MST, which provides a  
183 powerful alternative to the classical radioligand binding assay. Exploiting the protein's intrinsic  
184 fluorescence free in solution obviates the need for sample modifications like labelling or  
185 immobilization that might interfere or affect ligand binding. Using this approach, we confirmed  
186 the binding of hAhR to a known, *bona fide* ligands, including TCDD, FICZ, 1-HP and  
187 CH223191. Yet, compounds with an intrinsic fluorescence at or close to  $\lambda_{ex} \sim 280$  nm cannot  
188 be tested with this method due to the overlapping fluorescence with the target protein. The  
189 direct fusion of the target protein to a fluorescent tag, e.g. GFP or RFP that can be specifically  
190 monitored at the Monolith NT.115 machine, would circumvent this limitation, make additional  
191 purification steps needless and thus allow measurements to be done directly in cell lysates<sup>28</sup>.

192        Though the obtained binding affinities for the individually tested ligands to the recombinant  
193 protein are slightly lower than the ones reported in the literature for the hAhR<sup>13,24,26</sup>, such  
194 differences are presumably explainable by missing endogenous factors that are likely to support  
195 ligand sensing of the cytosolic AhR, e.g. stabilizing effects of chaperones (HSP90, XAP2) in  
196 the unbound receptor state<sup>29,30</sup>. Moreover and of note, most of the literature-described binding



197 affinities were experimentally determined for the murine AhR, which is known to display an  
198 almost 10-fold higher binding affinity towards TCDD than human AhR<sup>31</sup>.

199 Finally, the considerable advantages of buffer independency and the short reaction times  
200 enable fast and reliable monitoring of AhR binding to a large number of small molecules,  
201 including exogenous AhR ligands, AhR inhibitors, and also to less stable compounds (e.g.  
202 FICZ), for which previous interaction studies with longer assay times have proven to be  
203 challenging<sup>18,24</sup>. Altogether, in addition to the implementation of this method in basic research  
204 for analyzing AhR-ligand interactions and the signalling pathway in more detail, the novel AhR  
205 binding assay presented here bears the potential for future drug/compound screenings.  
206 Ultimately, this will facilitate the discovery of potential selective modulators of this intriguing  
207 broad-spectrum receptor of high interest for HDT.

208

209

## 210 **Material and Methods**

### 211 **Resource availability/contact for Reagent and Resource sharing**

212 Further information and requests for resources and reagents should be directed to and will be  
213 fulfilled by the corresponding author, Pedro Moura-Alves  
214 ([pedro.mouraalves@ludwig.ox.ac.uk](mailto:pedro.mouraalves@ludwig.ox.ac.uk)) or by the co-correspondent author, Michael Kolbe  
215 ([michael.kolbe@cssb-hamburg.de](mailto:michael.kolbe@cssb-hamburg.de)).

216

### 217 **Ligands**

218 All compounds were obtained from commercial sources, solubilized in dimethyl sulfoxide  
219 (DMSO) and stored protected from light. 2,3,7,8-Tetrachlorodibenzo-p-dioxin (TCDD) was  
220 obtained from LGC Standard. [<sup>3</sup>H]TCDD diluted in ethanol was from Hartmann Analytic. 1-

221 hydroxyphenazine (1-HP) was purchased from TCI Europe N.V., 6-Formylindolo[3,2-  
222 b]carbazole (FICZ) and 2-Methyl-2H-pyrazole-3-carboxylic acid (2-methyl-4-o-tolylazo-  
223 phenyl)-amide (CH-223191) from Sigma-Aldrich. 1-HP, CH-223191 and FICZ were kept at  
224 RT, 4°C or -20°C, respectively.

225

## 226 **Plasmid construction and protein preparation**

227 For the recombinant expression in *E. coli*, a codon-optimized fragment of human *AhR* (UniProt  
228 ID: P35869) encompassing the bHLH-PAS A-PAS B domains (amino acid residues 23 to 475)  
229 was commercially synthesized (MWG Eurofins) and cloned into pET21b harbouring an N-  
230 terminal His<sub>6</sub>- and the *Yersinia*-derived flagellin subunit FleB (amino acid residues 54 to 332,  
231 UniProt ID: A1JSQ5) as expression tag, followed by an HRV 3C protease cleavage site. The  
232 resulting construct was confirmed by DNA sequencing. The pET30-EK/LIC mARNT  
233 expression plasmid encoding the murine ARNT residues 85 to 465 ( $\Delta$ 274-297, C256S,  $\Delta$ 351-  
234 358, UniProt ID: P53762) was a generous gift from Prof. Dr. Oliver Daumke (MDC Berlin).  
235 The amino acid sequences of the expression vectors are shown in Supplementary Fig. 4. Both  
236 plasmids were co-transformed into *E. coli* BL21(DE3) competent cells (Novagen). Bacteria  
237 were grown to an OD<sub>600</sub> of 0.8 in lysogenic broth (LB (Luria/Miller)) medium (Carl Roth)  
238 before the expression was induced with 0.5 mM isopropyl- $\beta$ -D-thiogalactopyranoside (IPTG,  
239 Sigma-Aldrich). Following overnight expression at 18°C, proteins were purified as described  
240 previously<sup>12,21</sup> (see also Supplementary Fig. 1). Shortly, pellets were lysed using an SLM  
241 Aminco Pressure Cell Press and the clarified lysate was applied onto a HisTALON Superflow  
242 column (Clontech). Bound proteins were eluted by applying an increasing imidazole  
243 concentration, buffer exchanged and N-terminal His<sub>6</sub>-tags were removed with HRV 3C  
244 protease (3C) overnight at 4°C. The cleaved protein complex was further purified on a HiTrap  
245 Heparin HP column (GE Healthcare), followed by size exclusion chromatography on a

246 Superdex 200 10/300 GL equilibrated in 20 mM HEPES pH 8.0, 200 mM NaCl, 5% glycerol,  
247 and 5 mM DTT. Peak fractions containing AhR-mARNT were pooled and concentrated using  
248 Amicon filter units (Millipore).

249 Mouse ARNT (residues 85-465) was expressed as N-terminal His<sub>6</sub>-fusion protein in *E. coli*  
250 BL21(DE3) and purified as described above for the heterodimer complex.

251

### 252 **Radioactive labelled TCDD competition**

253 Radioligand binding assays were performed as previously established<sup>13</sup>. Briefly, for saturation  
254 experiments, 0.5 mg/ml of purified AhR-ARNT or ARNT protein was diluted in MDEG buffer  
255 (25 mM MOPS, 1 mM DTT, 1 mM EDTA, 10% glycerol, 20 mM molybdate, pH 7.5) and  
256 incubated with increasing concentrations of radioactively labelled [<sup>3</sup>H]TCDD tracer. Reactions  
257 were supplemented with liver lysate of AhR-deficient mice (AhR<sup>-/-</sup>, C57BL/6 background) to  
258 a final protein concentration of 5 mg/ml to reduce unspecific binding and adsorption of the  
259 tracer to plastic surfaces. Liver lysates were prepared in MDEG buffer by homogenization  
260 using the gentleMacs Dissociator (Miltenyi Biotec), followed by ultracentrifugation at  
261 100,000xg and 4°C for 1h. Cytosolic fractions were collected, protein concentration  
262 determined by Bradford reaction (Protein Assay Kit, Pierce), and further diluted to a final  
263 protein concentration of 5 mg/ml in MDEG buffer. Binding reactions were incubated at 4°C  
264 for 24 h in order to ensure equilibrium conditions. Subsequently, 30 µl of a Norit A charcoal  
265 suspension (100 mg/ml equilibrated in MDEG buffer) was added into each 200 µl of the  
266 reaction mixture. Samples were kept on ice for 15 min and centrifuged for another 15 min at  
267 25,000xg and 4°C. Following this, 150 µl of the supernatant was carefully transferred and  
268 radioactivity was measured in a liquid scintillation counter (Tri-Carb 3110TR, PerkinElmer).  
269 All samples were measured in triplicate. For competition assays, a constant concentration of  
270 [<sup>3</sup>H]TCDD (4 nM final) was used, to which a serial dilution of unlabeled competitor molecule

271 dissolved in DMSO was added in excess. All subsequent steps were carried out as described  
272 above. The specific binding was defined as the difference of radioactivity between the reactions  
273 supplemented with the recombinant protein and AhR-deficient (Ahr<sup>-/-</sup>) mouse lysates. Analysis  
274 of the data and calculation of the binding constants  $K_d$  and  $B_{max}$  was performed with GraphPad  
275 Prism 7 by using a nonlinear regression fitting a saturation binding isotherm. For competition  
276 studies, the IC<sub>50</sub> values were obtained by fitting a one-site competitive binding equation to the  
277 experimental data.  $K_i$  values were derived from IC<sub>50</sub> using the Cheng-Prusoff equation<sup>32</sup>.

278

### 279 **Microscale Thermophoresis (MST)**

280 Microscale thermophoresis (MST) experiments were performed according to the  
281 manufacturer's instructions (NanoTemper Technologies GmbH) using a Monolith  
282 NT.LabelFree. In brief, 250 nM of purified AhR-ARNT proteins were diluted in assay buffer  
283 (20 mM HEPES pH 8.0, 200 mM NaCl, 5% glycerol, 5 mM DTT, and 0.1% Pluronic F-127)  
284 and incubated for 5 min, in the presence of a serial dilution of the different ligands (ligand  
285 solubilized in DMSO at a final constant concentration of 2%). After incubation, samples were  
286 filled into NT.LabelFree Zero Background MST Premium coated capillaries (NanoTemper  
287 Technologies GmbH) and measurements were taken, at a constant temperature of 22°C. MST  
288 traces were collected with an LED excitation power of 20% and an MST laser power of 20%  
289 and 40%. The MO.Control Analysis software (NanoTemper) was used to analyze the  
290 interaction affinity and the dissociation constant ( $K_d$ ) for each ligand using the  $K_d$  fit model.  
291 Changes in the normalized fluorescence ( $\Delta F_{norm}$  [%]) were plotted as a function of the ligand  
292 concentration.

293

### 294 **Mice handling for preparation of liver cell suspensions**

295 AhR-deficient mice (*Ahr*<sup>-/-</sup>, C57BL/6 background) were kindly provided by B. Stockinger  
296 (The Francis Crick Institute, London, United Kingdom). *Ahr*<sup>-/-</sup> mice were bred in the Max  
297 Planck Institute for Infection Biology mouse facility. Animal experiments were carried out  
298 according to institutional guidelines approved by the local ethics committee of the German  
299 authorities (Landesamt für Gesundheit und Soziales Berlin; Landesamt für Verbraucherschutz  
300 und Lebensmittelsicherheit, project number G0257/12). Liver were isolated from mice of 8–  
301 12 weeks of age following published protocols<sup>8</sup>.

302

### 303 **Quantification and statistical analysis**

304 Data fitting including baseline corrections, normalization, calculation of mean and error  
305 (SEM), and statistical tests were carried out in GraphPad Prism (version 7). The number of  
306 biological and technical replicates, as well as the entity plotted, are indicated in the figure  
307 legends. Data baseline correction and normalization, where applied, were indicated in the  
308 corresponding method section and the axis labels. No explicit power analysis was used.

309

### 310 **Data Availability**

311 The authors declare that this study did not generate or analyze a datasets/code.

312

## 313 References

- 314 1 Du, X., Li, Y., Xia, Y. L., Ai, S. M., Liang, J., Sang, P., Ji, X.L. & Liu, S.Q. Insights into  
315 Protein-Ligand Interactions: Mechanisms, Models, and Methods. *Int. J. Mol. Sci.* **17**, pii:  
316 E144 (2016).
- 317 2 Pattnaik, P. Surface plasmon resonance: applications in understanding receptor-ligand  
318 interaction. *Appl. Biochem. Biotechnol.* **126**, 79-92 (2005).
- 319 3 Pierce, M.M., Raman, C.S. & Nall, B.T. Isothermal titration calorimetry of protein-  
320 protein interactions. *Methods* **19**, 213-221 (1999).
- 321 4 Duhr, S. & Braun, D. Why molecules move along a temperature gradient. *Proc. Natl.*  
322 *Acad. Sci. U S A.* **103**, 19678-19682 (2006).
- 323 5 Seidel, S.A., Dijkman, P.M., Lea, W.A., van den Bogaart, G., Jerabek-Willemsen, M.,  
324 Lazic, A., Joseph, J.S., Srinivasan, P., Baaske, P., Simeonov, A., Katritch, I., Melo, F.A.,  
325 Ladbury, J.E., Schreiber, G., Watts, A., Braun, D. & Duhr, S. Microscale thermophoresis  
326 quantifies biomolecular interactions under previously challenging conditions. *Methods*  
327 **59**, 301-315 (2013).
- 328 6 Stockinger, B., Di Meglio, P., Gialitakis, M. & Duarte, J.H. The aryl hydrocarbon  
329 receptor: multitasking in the immune system. *Annu. Rev. Immunol.* **32**, 403-432 (2014).
- 330 7 Rothhammer, V. & Quintana, F.J. The aryl hydrocarbon receptor: an environmental  
331 sensor integrating immune responses in health and disease. *Nat. Rev. Immunol.* **19**, 184-  
332 197 (2019).
- 333 8 Moura-Alves, P., Faé, K., Houthuys, E., Dorhoi, A., Kreuchwig, A., Furkert, J., Barison,  
334 N., Diehl, A., Munder, A., Constant, P., Skrahina, T., Guhlich-Bornhof, U., Klemm, M.,  
335 Koehler, A.B., Bandermann, S., Goosmann, C., Mollenkopf, H.J., Hurwitz, R.,  
336 Brinkmann, V., Fillatreau, S., Daffe, M., Tümmler, B., Kolbe, M., Oschkinat, H., Krause,

- 337 G. & Kaufmann, S.H. AhR sensing of bacterial pigments regulates antibacterial defence.  
338 *Nature* **512**, 387-392 (2014).
- 339 9 Murray, I.A., Patterson, A.D. & Perdew, G.H. Aryl hydrocarbon receptor ligands in  
340 cancer: friend and foe. *Nat Rev Cancer* **14**, 801-814 (2014).
- 341 10 Moura-Alves, P., Puyskens, A., Stinn, A., Klemm, M., Gühlich-Bornhof, U., Dorhoi, A.,  
342 Furkert, J., Kreuchwig, A., Protze, J., Lozza, L., Pei, G., Saikali, P., Perdomo, C.,  
343 Mollenkopf, H.J., Hurwitz, R., Kirschhoefer, F., Brenner-Weiss, G., Weiner, J.,  
344 Oschkinat, H., Kolbe, M., Krause, G. & Kaufmann, S.H.E. Host Monitoring of Quorum  
345 Sensing During *Pseudomonas aeruginosa* Infection. *Science* **20**, 366(6472):eaaw1629  
346 (2019).
- 347 11 Puyskens, A. *et al.* Aryl Hydrocarbon Receptor Modulation by Tuberculosis Drugs  
348 Impairs Host Defense and Treatment Outcomes. *Cell Host Microbe* **27**, 238-248 e237,  
349 doi:10.1016/j.chom.2019.12.005 (2020).
- 350 12 Huang, N., Chelliah, Y., Shan, Y., Taylor, C.A., Yoo, S.H., Partch, C., Green, C.B.,  
351 Zhang, H. & Takahashi, J.S. Crystal structure of the heterodimeric CLOCK:BMAL1  
352 transcriptional activator complex. *Science* **337**, 189-194 (2012).
- 353 13 Bradfield, C.A. & Poland, A. A competitive binding assay for 2,3,7,8-  
354 tetrachlorodibenzo-p-dioxin and related ligands of the Ah receptor. *Mol. Pharmacol.* **34**,  
355 682-688 (1988).
- 356 14 Pandini, A., Soshilov, A.A., Song, Y., Zhao, J., Bonati, L. & Denison, M.S. Detection of  
357 the TCDD binding-fingerprint within the Ah receptor ligand binding domain by  
358 structurally driven mutagenesis and functional analysis. *Biochemistry* **48**, 5972-5983  
359 (2009).

- 360 15 Wilkinson, I.V.L., Perkins, K.J., Dugdale, H., Moir, L., Vuorinen, A., Chatzopoulou,  
361 M., Squire, S.E., Monecke, S., Lomow, A., Geese, M., Charles, P.D., Burch, P., Tinsley,  
362 J.M., Wynne, G.M., Davies, S.G., Wilson, F.X., Rastinejad, F., Mohammed, S., Davies,  
363 K.E. & Russell, A.J. Chemical Proteomics and Phenotypic Profiling Identifies the Aryl  
364 Hydrocarbon Receptor as a Molecular Target of the Urothelin Modulator Ezutromid.  
365 *Angew. Chem. Int. Ed. Engl.* **59**, 2420–2428 (2020).
- 366 16 Brown, M.R., Garside, H., Thompson, E., Atwal, S., Bean, C., Goodall, T., Sullivan, M.  
367 & Graham, M.J. From the Cover: Development and application of a dual rat and human  
368 AHR activation assay. *Toxicol. Sci.* **60**, 408-419 (2017).
- 369 17 Bisson, W.H., Koch, D.C., O'Donnell, E.F., Khalil, S.M., Kerkvliet, N.I., Tanguay, R.L.,  
370 Abagyan, R. & Kolluri, S.K. Modeling of the aryl hydrocarbon receptor (AhR) ligand  
371 binding domain and its utility in virtual ligand screening to predict new AhR ligands. *J.*  
372 *Med. Chem.* **52**, 5635-5641 (2009).
- 373 18 Fan, M.Q., Bell, A.R., Bell, D.R., Clode, S., Fernandes, A., Foster, P.M., Fry, J.R., Jiang,  
374 T., Loizou, G., MacNicoll, A., Miller, B.G., Rose, M., Shaikh-Omar, O., Tran, L. &  
375 White, S. Recombinant expression of aryl hydrocarbon receptor for quantitative ligand-  
376 binding analysis. *Anal. Biochem.* **384**, 279-287 (2009).
- 377 19 Coumailleau, P., Poellinger, L., Gustafsson, J.A. & Whitelaw M.L. Definition of a  
378 minimal domain of the dioxin receptor that is associated with hsp90 and maintains wild  
379 type ligand binding affinity and specificity. *J. Biol. Chem.* **270**, 25291-25300 (1995).
- 380 20 Wu, D., Su, X., Potluri, N., Kim, Y. & Rastinejad, F. NPAS1-ARNT and NPAS3-ARNT  
381 crystal structures implicate the bHLH-PAS family as multi-ligand binding transcription  
382 factors. *Elife* **5** pii: e18790 (2016).



- 383 21 Schulte, K.W., Green, E., Wilz, A., Platten, M. & Daumke, O. Structural basis for aryl  
384 hydrocarbon receptor-mediated gene activation. *Structure* **25**, 1025-1033 (2017).
- 385 22 Vonderviszt, F., Aizawa, S. & Namba, K. Role of the disordered terminal regions of  
386 flagellin in filament formation and stability. *J. Mol. Biol.* **221**, 1461-1474 (1991).
- 387 23 Zhao, B., Degroot, D.E., Hayashi, A., He, G. & Denison, M.S.: CH223191 is a ligand-  
388 selective antagonist of the Ah (Dioxin) receptor. *Toxicol. Sci.* **117**, 393-403 (2010).
- 389 24 Wei, Y.D., Helleberg, H., Rannug, U. & Rannug, A. Rapid and transient induction of  
390 CYP1A1 gene expression in human cells by the tryptophan photoproduct 6-  
391 formylindolo[3,2-b]carbazole. *Chem. Biol. Interact.* **110**, 39-55 (1998).
- 392 25 Zhang, C., Creech, K.L., Zuercher, W.J. & Willson, T.M. Gram-scale synthesis of FICZ,  
393 a photoreactive endogenous ligand of the aryl hydrocarbon receptor. *Sci. Rep.* **9**, 9982  
394 (2019).
- 395 26 Poland, A., Glover, E. & Kende, A.S. Stereospecific, high affinity binding of 2,3,7,8-  
396 tetrachlorodibenzo-p-dioxin by hepatic cytosol. Evidence that the binding species is  
397 receptor for induction of aryl hydrocarbon hydroxylase. *J. Biol. Chem.* **251**, 4936-4946  
398 (1976).
- 399 27 Seidel, S.A., Wienken, C.J., Geissler, S., Jerabek-Willemsen, M., Duhr, S., Reiter, A.,  
400 Trauner, D., Braun, D. & Baaske, P. Label-free microscale thermophoresis discriminates  
401 sites and affinity of protein-ligand binding. *Angew. Chem. Int. Ed. Engl.* **51**: 10656-10659  
402 (2012).
- 403 28 Khavrutskii, L., Yeh, J., Timofeeva, O., Tarasov, S.G., Pritt, S., Stefanisko, K. &  
404 Tarasova, N. Protein purification-free method of binding affinity determination by  
405 microscale thermophoresis. *J. Vis. Exp.* **78** (2013).

- 406 29 Meyer, B.K. & Perdew G.H. Characterization of the AhR-hsp90-XAP2 core complex  
407 and the role of the immunophilin-related protein XAP2 in AhR stabilization.  
408 *Biochemistry* **38**, 8907-8917 (1999).
- 409 30 Pongratz, I., Mason, G.G. & Poellinger, L. Dual roles of the 90-kDa heat shock protein  
410 hsp90 in modulating functional activities of the dioxin receptor. Evidence that the dioxin  
411 receptor functionally belongs to a subclass of nuclear receptors which require hsp90 both  
412 for ligand binding activity and repression of intrinsic DNA binding activity. *J. Biol.*  
413 *Chem.* **267**, 13728-13734 (1992).
- 414 31 Flaveny, C.A. & Perdew, G.H. Transgenic Humanized AHR Mouse Reveals Differences  
415 between Human and Mouse AHR Ligand Selectivity. *Mol. Cell. Pharmacol.* **1**, 119-123  
416 (2009).
- 417 32 Cheng, Y. & Prusoff, W.H. Relationship between the inhibition constant (K<sub>1</sub>) and the  
418 concentration of inhibitor which causes 50 per cent inhibition (I<sub>50</sub>) of an enzymatic  
419 reaction. *Biochem. Pharmacol.* **22**, 3099–3108 (1973).
- 420

## 421 **Acknowledgements**

422 The authors acknowledge those who have provided tools and materials for this work. Brigitta  
423 Stockinger (The Francis Crick Institute, London, UK) for the *Ahr*<sup>-/-</sup> mice. Expression plasmid  
424 pET30-EK/LIC-ARNT was a gift from Oliver Daumke and Kathrin Schulte (Max Delbruck  
425 Center, Berlin, Germany). We acknowledge the lab of Rainer Haag (Freie Universität Berlin,  
426 Berlin, Germany) for providing access to Monolith NT.LabelFree, Maria Garcia Alai, Ioana  
427 Maria Nemtanu and Janina Hinrichs (European Molecular Biology Laboratory, Hamburg,  
428 Germany) for technical assistance and Juana de Diego (Center for Structural Systems Biology,  
429 Hamburg, Germany) for scientific discussions.

430 This work was generously supported by intramural funding of the Max Planck Society to  
431 SHEK, by the International Max Planck Research School for Infectious Diseases and  
432 Immunology (IMPRS-IDI) and by iNEXT, infrastructure for NMR, EM and X-rays for  
433 Translational Research, project number 653706, funded by the Horizon 2020 programme of  
434 the European Union.

435

## 436 **Author contributions**

437 AS, SHEK, PM-A and MK conceived and AS and MK designed the study. AS designed and  
438 performed the experiments and data analysis. AS and JF performed the radioligand binding  
439 studies. AS, PM-A, MK wrote the manuscript. All authors commented on the paper.

440

## 441 **Declaration of interests**

442 The authors declare no competing interests. Correspondence and requests for materials should  
443 be addressed to [pedro.mouraalves@ludwig.ox.ac.uk](mailto:pedro.mouraalves@ludwig.ox.ac.uk) or [michael.kolbe@cssb-hamburg.de](mailto:michael.kolbe@cssb-hamburg.de).

444 **Figure legends**

445 **Figure 1. Verification of the ligand-binding properties of the recombinant AhR-ARNT**

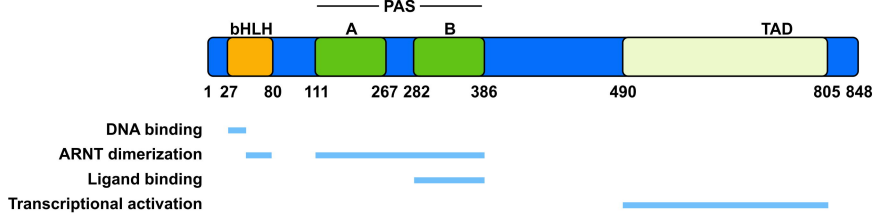
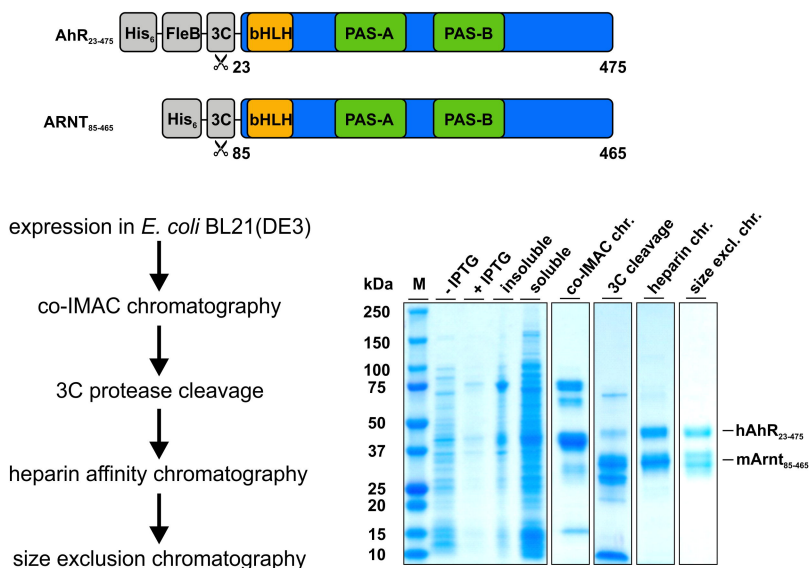
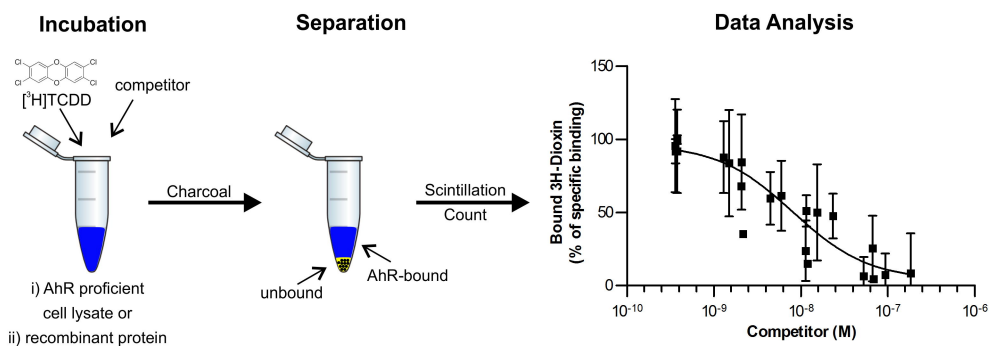
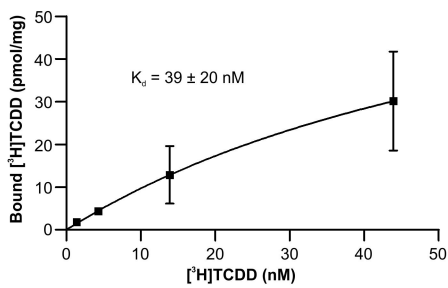
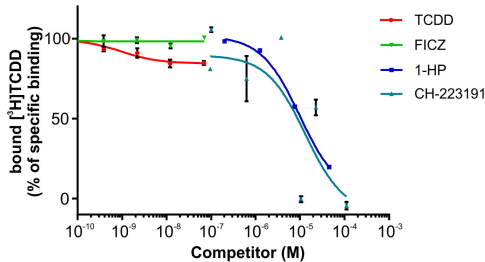
446 **by radioligand binding assay.** (a) Functional domains of the human hAhR. Numbers indicate  
447 amino acid residues displaying the relative domain boundaries. (b) Schematic representation  
448 of the AhR-ARNT protein complex purification. Both proteins were co-expressed in *E. coli*  
449 BL21(DE3) and purified in a 3-step purification process. Samples from different steps of the  
450 purification were analyzed by SDS-PAGE and Coomassie staining. The theoretical molecular  
451 weight of the AhR and ARNT after cleavage with 3C is 51 and 40 kDa, respectively. (c)  
452 Principle of the radioligand binding assay. AhR-deficient and -proficient liver lysates were  
453 incubated with radioactively labelled [<sup>3</sup>H]TCDD and, in case of competition assays, in  
454 presence of increasing concentrations of unlabeled competitor ligands. After incubation,  
455 charcoal was added to remove unbound tracer molecules and radioactivity of the supernatant  
456 was measured. Specific binding was defined as the difference of radioactivity between extracts  
457 supplemented with recombinant AhR-ARNT and AhR-deficient lysates. (d) Saturation binding  
458 analysis of the purified AhR-ARNT receptor complex incubated with different concentrations  
459 of radioactively labelled [<sup>3</sup>H]TCDD. (e) Concentration-dependent displacement of [<sup>3</sup>H]TCDD  
460 from AhR-ARNT co-incubated with increasing concentrations of unlabeled competitor  
461 ligands. After 24 h, radioactivity in the supernatants was measured and competitive binding  
462 after NSB-subtraction was calculated. Data are mean ± SD of two independent experiments  
463 performed with triplicates.

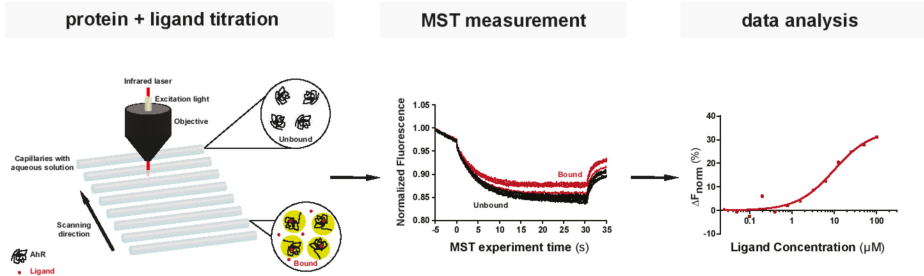
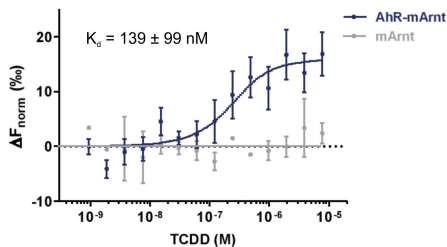
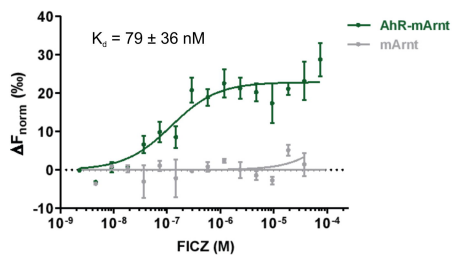
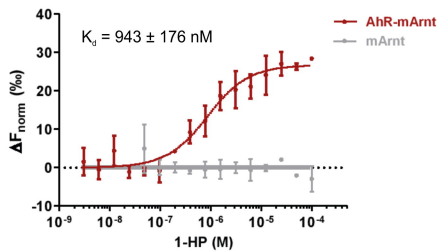
464

465 **Figure 2. Suitability of MST as a sensitive method to determine AhR-ligand binding**

466 **affinities.** (a) The basic principle of an MST ligand binding experiment. The thermophoretic  
467 movement of the intrinsically fluorescent protein in the presence of increasing concentrations  
468 of a non-fluorescent ligand is analysed. In the case of binding (bound, red traces),  
469 thermophoresis will differ from the unbound state and will result in a gradual change in the  
470 recorded MST traces. Plotting the changes in the normalized fluorescence as a function of the  
471 ligand concentration will yield a binding curve that can be fitted to calculate the binding  
472 affinities. (b-e) Binding of the prototypic ligand TCDD (b), the endogenous ligand FICZ (c),  
473 the bacterial pigment 1-HP (d) and the AhR inhibitor CH-223191 (e) to 250 nM recombinant  
474 AhR-ARNT complex was analysed with label-free MST (coloured lines). To verify that the  
475 measured interaction was exclusive for AhR, we examined binding to separately purified

476 ARNT (grey line). Error bars represent the  $\pm$  SD of each tested ligand concentration calculated  
477 from three independent experiments.  
478

**a****b****c****d****e**

**a****b****c****d****e**